SECURITY CLASSIFICATION OF THIS PAGE

REPORT DOCUMENTATION PAGE

DTIC FILE COPY

AD-A227 224

1a REPORT SECURITY CLASSIFICATION UNCLASSIFIED	1b. RESTRICTIVE MARKINGS
2a. SECURITY CLASSIFICATION AUTHORITY	3 DISTRIBUTION/AVAILABILITY OF REPORT Approved for public release
2b. DECLASSIFICATION/DOWNGRADING SCHEDULE	
4. PERFORMING ORGANIZATION REPORT NUMBER(S) Number 4	5 MONITORING ORGANIZATION REPORT NUMBER(S) N00014-89-J-1197
6a. NAME OF PERFORMING ORGANIZATION High Temperature Gasdynamics Lab Stanford University 6b OFFICE SYMBOL (If applicable)	7a. NAME OF MONITORING ORGANIZATION Office of Naval Research Dr. Robert Schwartz
6c ADDRESS (City, State, and ZIP Code) Mechanical Engineering Dept. Stanford, CA 94305-3032	7b. ADDRESS (City, State, and ZIP Code) Code 373 Naval Weapons Center China Lake, CA 93555-6001
8a. NAME OF FUNDING/SPONSORING ORGANIZATION Office of Naval Research 8b. OFFICE SYMBOL (If applicable)	9. PROCUREMENT INSTRUMENT IDENTIFICATION NUMBER
8c. ADDRESS (City, State, and ZIP Code) 800 North Quincy Street Arlington, VA 22217-5000	10 SOURCE OF FUNDING NUMBERS PROGRAM ELEMENT NO. / PROJECT NO. / TASK NO. / WORK UNIT NO

DTIC ELECTE OCT 04 1990 S E D

11 TITLE (Include Security Classification)
An Investigation of Diamond Synthesis in an Oxygen-Acetylene Diffusion Flame

12 PERSONAL AUTHOR(S) M. A. Cappelli

13a. TYPE OF REPORT	13b. TIME COVERED	14 DATE OF REPORT (Year, Month, Day)	15 PAGE COUNT
Technical	FROM _____ TO _____	September, 1990	5

16 SUPPLEMENTARY NOTATION

17 COSATI CODES			18. SUBJECT TERMS (Continue on reverse if necessary and identify by block number)
FIELD	GROUP	SUB-GROUP	

19 ABSTRACT (Continue on reverse if necessary and identify by block number)

Diamond synthesis is demonstrated in an oxygen-acetylene diffusion flame. The acetylene flame is diluted with argon to suppress sooting tendencies and is sustained and stabilized by overventilation with a surrounding oxygen flow. The result is a relatively cold flame, and the carbon film is deposited on a *free-standing* silicon wafer without the need for substrate cooling. Deposition patterns observed so far are nonuniform, with diamond deposited within a small annular ring surrounding a predominantly amorphous carbon film. Particle growth rates observed are in the range of 20-50 μm/hour, and deposit patterns are qualitatively similar to those observed in premixed oxygen-acetylene flames, however, unlike in premixed flame deposition, the temperature distribution appears to be much more nonuniform, with heat generated primarily at the diffusion flame boundary.

20 DISTRIBUTION/AVAILABILITY OF ABSTRACT	21 ABSTRACT SECURITY CLASSIFICATION	
☒ UNCLASSIFIED/UNLIMITED ☐ SAME AS RPT. ☐ DTIC USERS	Unclassified	
22a NAME OF RESPONSIBLE INDIVIDUAL	22b TELEPHONE (Include Area Code)	22c. OFFICE SYMBOL

DD FORM 1473, 84 MAR 83 APR edition may be used until exhausted
All other editions are obsolete

SECURITY CLASSIFICATION OF THIS PAGE

AN INVESTIGATION OF DIAMOND SYNTHESIS IN AN OXYGEN-ACETYLENE DIFFUSION FLAME

M. A. CAPPELLI
High Temperature Gasdynamics Laboratory, Stanford University, Stanford, CA 94305

ABSTRACT

Diamond synthesis is demonstrated in an oxygen-acetylene diffusion flame. The acetylene flame is diluted with argon to suppress sooting tendencies and is sustained and stabilized by overventilation with a surrounding oxygen flow. The result is a relatively cold flame, and the carbon film is deposited on a *free-standing* silicon wafer without the need for substrate cooling. Deposition patterns observed so far are nonuniform, with diamond deposited within a small annular ring surrounding a predominantly amorphous carbon film. Particle growth rates observed are in the range of 20-50 μm/hour, and deposit patterns are qualitatively similar to those observed in premixed oxygen-acetylene flames, however, unlike in premixed flame deposition, the temperature distribution appears to be much more nonuniform, with heat generated primarily at the diffusion flame boundary.

INTRODUCTION

Diamond film synthesis at low pressures in plasma activated environments is now common practise [1,3]. At pressures below 100 torr, growth rates of approximately 1 μm/hour are routinely achieved. Growth rates well in excess of 100 μm/hour have been demonstrated over limited areas (~ 1 cm^2) [4,5], and over relatively large areas (10-20 cm^2) [6] in atmospheric pressure discharges.

Recently, there has been an increase in activity in the use of combustion environments for diamond chemical vapor deposition [7-11]. This approach is particularly appealing, in that the reactive growth species are produced by the self-sustained combustion process, and that the results obtained so far are best at atmospheric pressures, employing a conventional welding or cutting torch operating with a slightly fuel rich mixture of oxygen and acetylene [10]. Growth rates of 100-150 μm/hour have been reported [7], in some cases, of well faceted crystals that are nearly optically transparent [12]. The deposit morphologies and growth rates observed display a spatial pattern that is nonuniform [13], reflecting the strong radial gradients associated with the oxygen-acetylene flame in stagnation flow. For flow rates of approximately 2 l/min and substrate to nozzle separations D ~ 0.3 - 1 cm, it is often observed [10,13] that diamond is deposited in annular rings, with little or no carbon deposited on the substrate in the central region near the flame axis. This result has been attributed to the inherent structure of a fuel rich premixed flame (free burning) in an oxygen environment [9,10]. In essence, the secondary flame zone represents a *diffusion flame*, with unreacted fuel (diluted with products of the primary flame reaction) burning with oxygen diffusing from the surrounding room air.

That the diffusion flame region of a fuel rich premixed flame can represent an alternative source of radicals likely to participate in diamond growth suggests the direct use of a diffusion-type burner for further investigation. Such an approach has its advantages in that it can be designed to significantly reduce the overall heat flux to the substrate in comparison to premixed flame deposition. The difficulty in overcoming the excess heat flux (~ 2kW/cm^2) in premixed flame deposition has been discussed previously [10,11]. Also, a diffusion flame is safer to operate with hydrogen as an additive to the hydrocarbon-based fuel.

In this paper, we report on the use of a single-nozzle diffusion flame for diamond synthesis. Our preliminary results are consistent with the observations of annular ring type deposit structures observed in premixed flame deposition. These results are used to further interpret the results of Oakes et al [13], particularly, the effects of hydrogen addition to premixed oxygen-acetylene flames on the resulting deposit structure.

BACKGROUND

In order to help us understand the chemical nature of the post primary flame zone in premixed oxygen-acetylene flames (often referred to as the acetylene feather), we have constructed a one-dimensional flame kinetics model. This model is used to describe the time evolution of the chemistry within a volume element of fluid traveling along a streamline from the torch nozzle. We use it here, to provide insight as to the composition of the post primary flame as we approach the diffusion (secondary) flame boundary, at which remaining fuel (C_2H_x) reacts with oxygen diffusing in from the surrounding atmosphere. The model solves the coupled energy and species conservation equations for a prescribed temperature-time history and is simplified by neglecting diffusive transport. We employ an elementary reaction set that has been used to describe the chemistry in methane-air flames [14]. The volumetric reaction rates are calculated using the subroutine package CHEMKIN [15]. We assume that the temperature rises from 800K at the flame nozzle exit to approximately 3300K (the adiabatic flame temperature of CO and O_2 mixtures) in 1 ms. For O_2/C_2H_2 flow ratios R, in the range of 0.8-1.0, much of the acetylene and essentially all of the oxygen are consumed within 0.2 ms, this representing the action of the primary flame (Figure 1). The acetylene feather is interpreted as the region following the primary flame, rich in C_2H_x species. At a time t = 0.8 ms (a distance of approximately four times the length of the primary cone away from the primary cone tip) the values of the mole fractions computed for the stable species CO, H_2 and C_2H_2 are 0.55, 0.2 and 0.07 respectively. These are somewhat consistent (within a factor of two) with the mass sampling measurements of Matsui et al [16] at comparable distances from the primary flame tip, within the acetylene feather (see also Figure 1).

The relatively small amount of acetylene in comparison to the CO, H_2O and H_2 in the post primary flame zone represents a hydrocarbon fuel dilution of approximately 1:10. Our calculations suggests that if we wish to simulate to some extent the secondary flame present in the premixed oxygen-acetylene flame, one obvious approach is to ignite a mixture of CO, H_2O, H_2 and C_2H_2 in the proportions computed, in a conventional *diffusion* flame, with this diluted fuel mixture burning with entrained oxygen. Recognizing that CO and H_2O are relatively inert at the temperatures of interest (2000-3000K), in the experiments described below, we have substituted argon for all species other than acetylene.

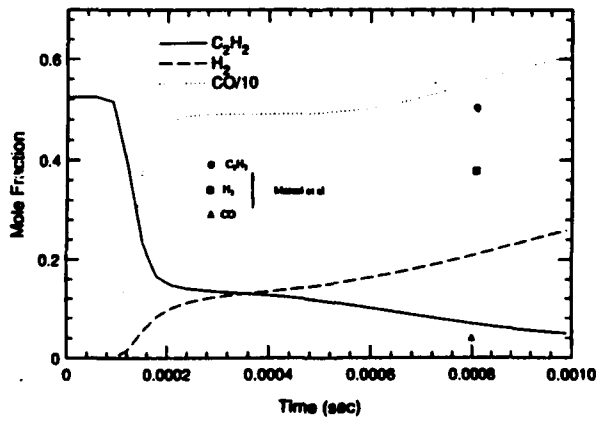

Figure 1. Results of one dimensional kinetic model for R = 1.1. The curves show the variation in the CO, C_2H_2, and H_2 species mole fraction with time. Experimental values (Ref. 16) are shown for comparison.

RESULTS

The diffusion flame facility consisted primarily of a standard brazing torch fitted with a number one tip, similar to that employed for studies of premixed oxygen-acetylene flame deposition [10]. The primary difference of course, is that only acetylene and argon mixtures pass through the torch nozzle, with oxygen provided as a co-flow as illustrated in Figure 2. Volumetric flow rates were monitored with calibrated rotometers. The total gas flow rate was approximately 1.5 l/min, with an acetylene to argon flow ratio (fuel dilution) of approximately 0.6. Sustaining dilution ratios of less than 0.6 was difficult, as the torch became unstable, with flame lifting leading to flame extinction.

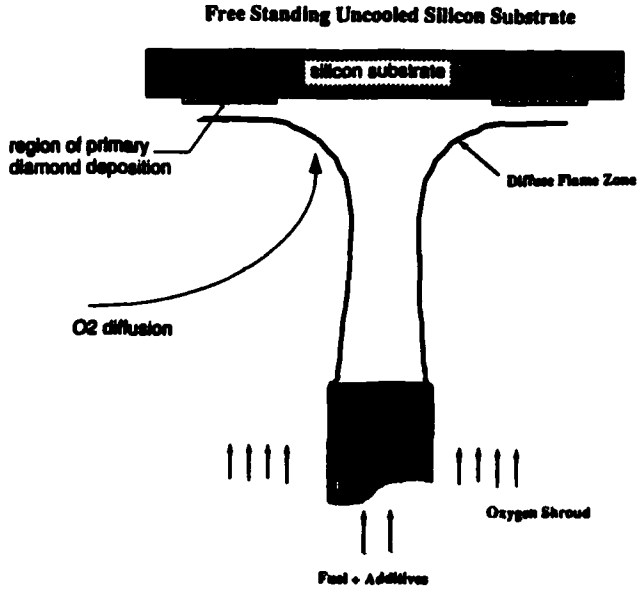

Figure 2. Schematic diagram of the diffusion flame deposition process. Note that the silicon wafer is free standing as a result of the reduced heat load.

The flame generated was blue to green in appearance, with little or no yellow emission that is characteristic of the onset of sooting in acetylene flames. Although the temperature of the flame was not measured, the fact that a *free standing* wafer can be positioned approximately 1 cm above the nozzle without damage or significant heating above 1200K indicates that the flame temperature is substantially less than that of the premixed flame at comparable flow rates. This is not surprising, as it is well known that in premixed flames, a vast amount of the heat is released within the primary flame zone. In our case here, essentially all the heat is released at the diffusion flame zone, and the adiabatic flame temperature is expected to be significantly lower than that of a stoichiometric premixed flame due to the significant argon dilution. The brightness temperature of the substrate as measured by optical pyrometry, indicated a substantial radial variation. As expected, the temperature was a maximum (approximately 1200K at the location where the diffusion flame intersected the silicon substrate. Temperatures near the center of the deposit were to low too measure by this procedure.

Run durations of 15 minutes resulted in deposit morphologies that are qualitatively similar to what was observed with premixed flames [10], with one exception; thin (~ 5 μm thick) semi-transparent film was deposited within a 2 mm diameter region at the deposit center. We shall refer to this region in the following discussion as region I. The film in this region has no distinct features when viewed under an electron microscope. This region is surrounded by a darker ring (region II) approximately 500 μm wide that is grey in appearance. Region II corresponds to the location of the intersection of the diffusion flame with the substrate surface. The film in both region I and region II often delaminated from the substrate surface upon cooling, suggesting a substantial difference in thermal expansion

between it and the silicon substrate. At this point, it is difficult to say wether the films are in tension or compression prior to delamination.

Distinctly faceted diamond crystals are found to grow in the outer portion of this ring within a narrow region approximately 50-100 μm wide (region III). A scanning electron microscope (SEM) image of the transition from region II to region III is displayed in Figure 3. This sample was intentionally *not* coated with gold film in SEM preparation in order to illustrate the transition from poorly conducting to well insulating crystals, evident from the charging of the crystals in moving from region II to region III.

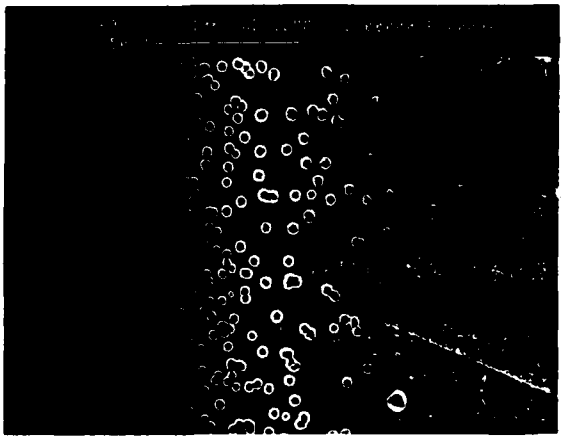

Figure 3. SEM photograph of the deposit showing the boundary between region II (predominantly amorphous carbon) and region III (diamond).

DISCUSSION

The structure and nature of the film deposited in regions I and II is yet to be determined. Raman analysis of the carbon film deposited within these regions indicate a structure very similar to that observed by Howard et al [17], in the synthesis of diamond powder via plasma enhanced combustion of oxygen-acetylene mixtures. Representative Raman scans for the two regions are displayed in Figures 4a and 4b. The broad (~ 80 cm^{-1} wide) peak very near the expected location of the Raman shift associated with the first order principal phonon mode in natural diamond (1332 cm^{-1}) has been interpreted as representing disordered sp_2 bonding [18]. This interpretation is based on the similarity between the observed spectra from regions I and II, and the spectra of three-coordinated amorphous and diamond-like carbon. This result is not surprising, in that the region in the gas phase immediately above region I on the surface is expected to be starved of atomic and molecular oxygen. It is likely to consist of primarily acetylene and argon, with some reaction products and intermediates (i.e., OH, H_2O, CO etc.) resulting from species diffusion from the diffusion flame zone. Most of the reactive intermediates likely to participate in diamond growth will be produced at this diffusion flame zone. The OH and (perhaps H) radicals are expected to play a major role in the etching of graphite and non-diamond carbon [19], and possibly in diamond growth itself. The transition between region

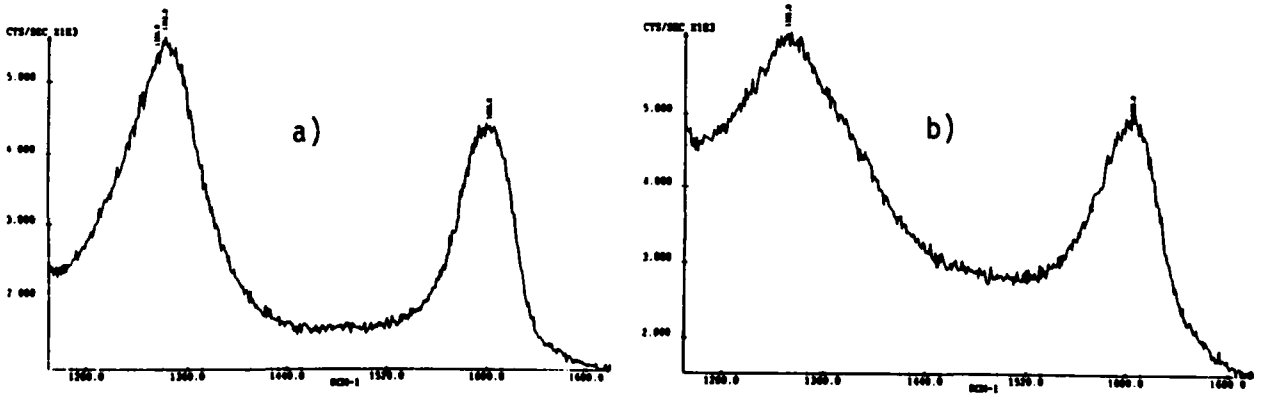

Figure 4. Raman spectrum of (a) deposit in region I and (b) deposit in region II

II and region III is interpreted as resulting from the transition between OH production via the reaction O_2(diff) + H -> OH + O, and OH consumption via C_2H_2 (fuel) + OH -> C_2H + H_2O, in the adjacent gas phase environment. A number of intermediate reactions will take place to further oxidize the hydrocarbon fragments and replenish the atomic hydrogen pool.

CONCLUSIONS

Confirmation that diamond particles can be synthesized in a conventional diffusion flame allows us to go back and reinterpret the results of Oakes et al [13]. In that work, they investigated the spatial nature of the carbon deposited in a premixed oxygen-acetylene flame, and the sensitivity of the observed Raman peak at 1332 cm^{-1} (relative to the peak at 1580 cm^{-1}) to hydrogen addition. They found that although hydrogen addition to the flame dramatically improved the "quality" of the diamond at the center of the deposit, it made little difference to the quality of the deposit in the annular ring. This is consistent with our evidence that the annular ring so often observed in flame deposited diamond is due to reactive species transport from the diffusion flame zone. Any increase in atomic hydrogen in the post primary flame resulting from hydrogen addition to the oxygen-acetylene mixture, is likely to be small in comparison to the OH and H radicals produced as intermediates in the diffusion flame zone. The fact that hydrogen addition nonetheless does have an effect on the structure of the deposit near the flame axis, suggests that the overall deposit is a result of two processes : (i) reactive species transport from the primary flame zone, and (ii) transport from the diffusion flame zone. Definitive experiments to evaluate the actual contribution from the primary flame can be performed by studies of diamond growth with a premixed oxygen-acetylene flame in an inert environment.

ACKNOWLEDGMENTS

This work was supported in part by the Office of Naval Research. The author would like to acknowledge S. Woolridge for his assistance in the experiments and thank M. Pinneo of Crystallume Inc. for Raman analysis of the samples.

REFERENCES

1. K.A. Spear, J. Am. Cream. Soc. 72, 171 (1989).
2. J.C. Angus and C.C. Hayman, Science 241, 913 (1988).
3. W.A. Yarbrough and R. Messier, Science 247, 688 (1990).
4. F. Akatsuka, Y. Hirose, and K. Komaki, Jap. Journal Appl. Phys. 27, L1600 (1988).
5. S. Matsumoto, H. Hino, and T. Kobayashi, Appl. Phys. Lett. 51, 737 (1987).
6. M.A. Cappelli, T.G. Owano and C.H. Kruger, J. Mater. Res. (in press).
7. Y. Hirose, Abstract of the 1st Int. Conf. on New Diamond Sci. and Tech. (Japan New Diamond Forum, Tokyo, 1988) p.38.
8. L.M. Hanssen, W.A. Carrington, J.E. Butler and K.A. Snail, Mat. Lett. 7, 289 (1988).
9. Y. Hirose and M. Mitsuizumi, N. Diamond 4, 34 (1988).
10. M.A. Cappelli and P.H. Paul, J. Appl. Phys. 67, 2602 (1990).
11. P.G. Kosky and D.S. McAtee, Mater. Letters 8, 369 (1989).
12. Y. Hirose (private communication).
13. D.B. Oakes, J.E. Butler, K.A. Snail, W.A. Carrington, and L.M. Hanssen, J. Appl. Phys. (in press).
14. D. Seery and C.T. Bowman, Combust. Flame 14, 37 (1970).
15. R.J. Kee, J.A. Miller, and T.H. Jefferson, Sandia Report No. SAND80-8003 UC-4, July (1987).
16. Y. Matsui, A. Yuuki, M. Sahara, and Y. Hirose, Jap. Journal Appl. Phys. 28, 1718 (1989).
17. W. Howard, D. Huang, J. Yuan, M. Frenklach, K.E. Spear, R. Koba, and A.W. Phelps, J. Appl. Phys. 68, 1247 (1990).
18. D.S. Knight and W.B. White, J. Mater. Res. 4, 385 (1989).
19. D.E. Rosner, Annu. Rev. Mater. Sci. 2, 573 (1972).

IR DOMES DISTRIBUTION LIST

October 1988

Dr. W. Adler
General Research Inc.
P. O. Box 6770
Santa Barbara, CA 93160

R. A. Heinecke
Standard Telecommunication
Laboratories, Ltd.
London Road
Harlow, Essex CM17 9MA
England

Mr. D. Roy
Coors Porcelain Co.
Golden, CO 80401

Dr. Mufit Akinc
Mat'ls Science & Eng. Dept.
Iowa State University
110 Engineering Annex
Ames, IA 50011

Dr. Lisa C. Klein
Center for Ceramics Research
College of Engineering
Rutgers University
P. O. Box 909
Piscataway, NJ 08854

Dr. D. Roy
Mat'ls Science Lab
Pennsylvania State Univ.
University Park, PA 16802

Dr. H. E. Bennett
Code 38101
Naval Weapons Center
China Lake, CA 93555

Dr. P. Klocek
Texas Instruments
P. O. Box 660246
Dallas, TX 75266

Dr. J. Savage
Royal Signals & Radar Establishment
St. Andrews Road
Great Malvern, WORCS, WR14 3PS
ENGLAND

Dr. S. Block
Group Leader
Structural Chemistry
National Bureau of Standards
Gaithersburg, MD 20899

Dr. R. Messier
Pennsylvania State University
Materials Research Lab
University Park, PA 16802

Dr. A. Stacy
Chemistry Departament
Univ. of Calif. Berkeley
Berkeley, CA 94720

Dr. J. Burdett
Chemistry Department
University of Chicago
Chicago, IL 60637

Dr. G. Messing
Materials Research Department
Pennsylvania State University
University Park, PA 16802
(1 copy for distribution)

Dr. I. G. Talmy, Code R31
Naval Surface Weapons Center
White Oak Laboratory
Silver Spring, MD 20903

Dr. Mark A. Cappelli
Mechanical Engineering Dept.
Stanford University
Stanford, CA 94305

Dr. S. Musikant
General Electric Company
P. O. Box 8555
Philadelphia, PA 19101

Dr. R. Tustison
Raytheon Co., Research Div.
131 Spring Street
Lexington, MA 02173

Dr. J. A. Cox
Honeywell Systems & Research
Dept. MN 65-2600
3660 Technology Drive
Minneapolis, MN 55418

Dr. Dale Perry
U.S. Army Missile Command
Redstone Arsenal
Huntsville, AL 35807

Dr. W. White
Materials Research Lab
Pennsylvania State Univ.
University Park, PA 16802

Dr. B. Dunn
Materials Science & Eng. Dept.
Univ. of California, Los Angeles
Los Angeles, CA 90024

Dr. W. Pittman
AMSI-RD-AS-PM
Redstone Arsenal
Huntsville, AL 35898

Dr. A. Wold
Chemistry Department
Brown University
Providence, RI 02912

Naval Surface Weapons Ctr
10901 New Hampshire Ave
White Oak Laboratory

Dr. A. Harker
Rockwell International
P. O. Box 1085
1049 Camino Dos Rios
Thousand Oaks, CA 91360

Dr. R. Raj
Materials Science&Eng. Dept.
Cornell University
Ithaca, NY 14853

Capt. Ken L. Yates
AD/AFATL/AGA
Eglin AFB, FL 32542

Office of Naval Research
800 N. Quincy Street
Arlington, VA 22217
Attn:Code1113(H.Guard)
" " " " " " " "(D.Nelson)

Dr. D. C. Harris (Code 3854)
Naval Weapons Center
China Lake, CA 93555
(1 copy for distribution)

Dr. W. Rhodes
GTE Laboratories
40 Sylvan Road
Waltham, MA 02134

Defense Documentation Center
Cameron Station
Alexandria, VA 22314
(12)

Dr. R. W. Schwartz
Code 373
Naval Weapons Center
China Lake, CA 93555-6001

Naval Air Systems Cmd
1411 Jeff Davis Hwy.
Arlington, VA 22202
Attn:Code 931A (L.Sloter)

Scientific Advisor
Commandant of the
MarineCorps(CodeAX)
Washington,DC 20380

Office of Naval Technology
800 N. Quincy Street
Arlington, VA 22217
Attn:Code 0712(1) Code 0725 (1)